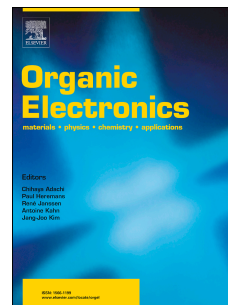


Accepted Manuscript

New naphthyridine-based bipolar host materials for thermally activated delayed fluorescent organic light-emitting diodes

Tzu-Chin Yeh, Jhen-De Lee, Lu-Yu Chen, Tanmay Chatterjee, Wen-Yi Hung, Ken-Tsung Wong



PII: S1566-1199(19)30168-5

DOI: <https://doi.org/10.1016/j.orgel.2019.04.003>

Reference: ORGELE 5197

To appear in: *Organic Electronics*

Received Date: 15 January 2019

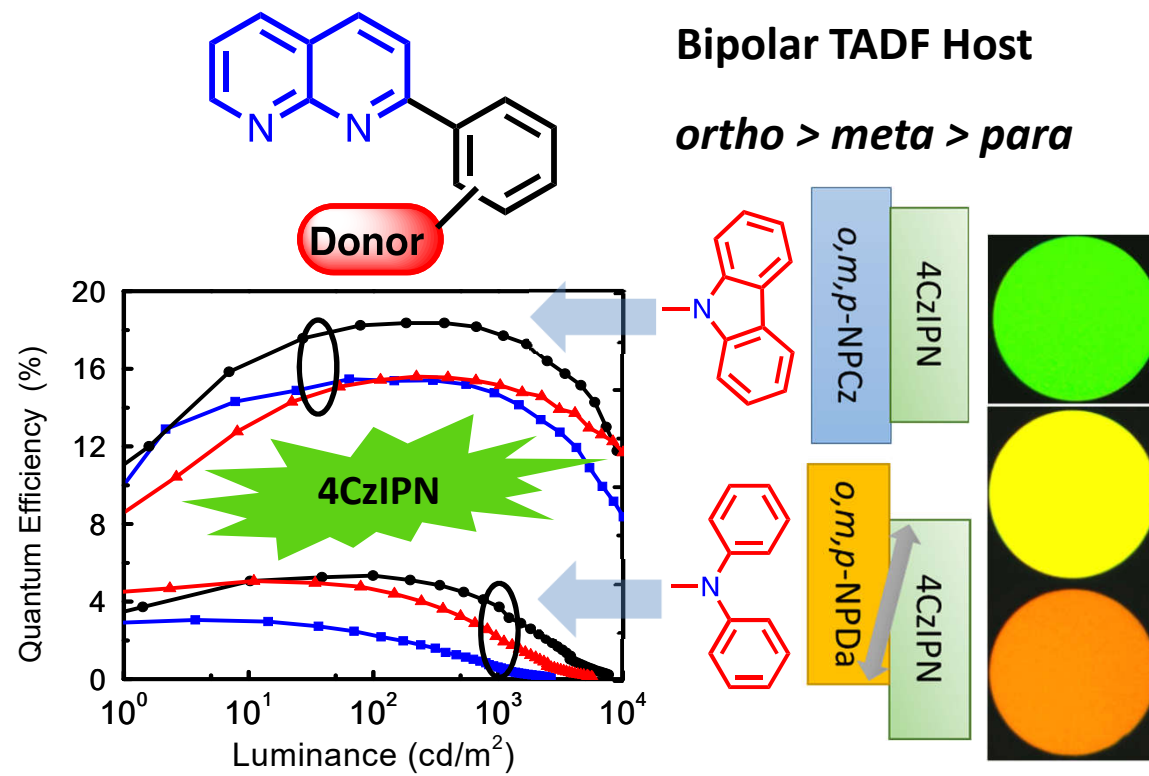
Revised Date: 12 March 2019

Accepted Date: 2 April 2019

Please cite this article as: T.-C. Yeh, J.-D. Lee, L.-Y. Chen, T. Chatterjee, W.-Y. Hung, K.-T. Wong, New naphthyridine-based bipolar host materials for thermally activated delayed fluorescent organic light-emitting diodes, *Organic Electronics* (2019), doi: <https://doi.org/10.1016/j.orgel.2019.04.003>.

This is a PDF file of an unedited manuscript that has been accepted for publication. As a service to our customers we are providing this early version of the manuscript. The manuscript will undergo copyediting, typesetting, and review of the resulting proof before it is published in its final form. Please note that during the production process errors may be discovered which could affect the content, and all legal disclaimers that apply to the journal pertain.

TOC graphic



New Naphthyridine-based Bipolar Host Materials for Thermally Activated Delayed Fluorescent Organic Light-Emitting Diodes

Tzu-Chin Yeh^a, Jhen-De Lee^b, Lu-Yu Chen^b, Tanmay Chatterjee^a, Wen-Yi Hung^{*b,c} and Ken-Tsung Wong^{*a,d}

^a Department of Chemistry, National Taiwan University, Taipei 106, Taiwan

^b Institute of Optoelectronic Sciences, National Taiwan Ocean University, Keelung 202, Taiwan

^c Center of Excellence for Ocean Engineering, National Taiwan Ocean University, Keelung 202, Taiwan

^d Institute of Atomic and Molecular Science, Academia Sinica, Taipei 10617, Taiwan

Corresponding authors:

W.-Y. Hung (wenhung@mail.ntou.edu.tw),

K.-T. Wong (kenwong@ntu.edu.tw)

Abstract

A series of bipolar host materials, namely, *o*-, *m*-, *p*-NPCz and *o*-, *m*-, *p*-NPDa, composing of electron-transporting naphthyridine (NP) and phenylene bridge with ortho-, meta-, and para-substituted hole-transporting carbazole (Cz)/diphenylamine (Da) were synthesized and characterized. By adjusting the linkage topology, the physical properties are subtly tuned. The characteristics of devices employing these new bipolar hosts with green thermally activated delayed fluorescence (TADF) emitter 1,2,3,5-tetrakis(carbazol-9-yl)-4,6-dicyanobenzene (4CzIPN) employed as emitter were investigated under the same device structure. Among these hosts, carbazole-based NPCz can perform efficient energy transfer from the host to the dopant and better exciton confinement in the emitting layer due to higher triplet energy and deeper HOMO/LUMO level than those of diphenylamine-based NPDa.

The device with *o*-NPCz as bipolar host exhibits the best device performance with external quantum efficiency of 18.4% and low efficiency roll-off. However, *o*-, *m*-, *p*-NPDA with lower E_T and shallower HOMO levels than 4CzIPN exhibit inferior host to dopant energy transfer. Instead, the exciplex formation between host and 4CzIPN, which was verified by TRPL, led the resulting EL spectra of the NPDA-based devices broad with yellow to orange emissions.

Keywords: TADF, bipolar host, naphthyridine, carbazole, diphenylamine, exciplex

1. Introduction

High-performance organic light-emitting diodes (OLEDs) have been a subject of extensive research both in academia and in industry for the last two decades. The utilization of thermally activated delayed fluorescence (TADF) in OLEDs for harnessing singlet as well as triplet excitons was for the first time brought about by Adachi et al. [1,2]. Organic materials which possess TADF characteristics are highly promising owing to their small singlet-triplet energy difference (ΔE_{ST}), which facilitates efficient reverse intersystem crossing (RISC) [3]. In principle, TADF OLEDs can lead to a maximum internal quantum efficiency of 100% [4,5], similar to phosphorescent OLED (PhOLED) employing Ir-based emitters. Analogous to PhOLEDs, the emitters in TADF-based OLEDs are generally homogeneously dispersed into a suitable host matrix so as to minimize de-excitation pathways, such as, triplet-triplet annihilation and/or concentration quenching, and thus, augment the efficacy of the device [6,7]. Thus, the astute choice of the host material is equally important to that of the emitter system. As host materials often take up the majority part (60–99%) in the emitting layer (EML), they are especially responsible for the power efficiency and turn-on voltage, thereby demonstrating their influence on the overall device performance [8]. In a typical TADF-based OLED, holes and electrons injected from the two opposing electrodes recombine in the EML to form excitons; whereby the EML comprise the wide-energy-gap host doped with a TADF emitter. This allows for efficient energy transfer from the host to the dopant and confinement of both singlet and triplet excitons within the TADF guest. The hosts for TADF-based OLEDs must generally fulfill certain critical requirements, such as, (a) the host should possess higher singlet and triplet (E_T) energies than the emitter for efficient energy transfer and thus confine the triplet excitons on the dopant, (b) the host should have suitably aligned energy levels for better charge injection, (c) the host material should have

bipolar properties (containing both hole-transporting and electron-transporting moieties) for better charge transport, which in turn, can aid in realizing much higher efficiency and smaller efficiency roll-offs [9-12]. Though three types of host materials (depending on charge transport properties) are employed in such OLEDs, viz., hole-transporting (p-type) [13], electron-transporting (n-type) [14,15], and bipolar (containing both p- and n-type functional moieties) [16], in which the bipolar hosts are found to be most successful [17,18]. However, the selection of the electron-transporting n-type units always remains the most essential but difficult part during the molecular design of bipolar hosts, since most of the n-type molecules have electron mobilities lower than the hole mobilities of p-type groups [19,20]. However, obtaining host materials with all the above properties are still a challenge. Thus, the host materials should be carefully designed so that the E_T , frontier orbital (HOMO/LUMO) levels and other parameters are well balanced with easy charge injection and transportation, rendering an efficient energy transfer to the dopant feasible and consequently an improved device performance.

Thus, it is also evident that host materials play a vital role in the photophysics of TADF emitters [21-23]. As the emitter is dispersed into the host matrix, therefore the host acts as a solid state solvent and thus, the various excited states (for example, local excited and charge transfer states etc.) are affected differently based on the polarity of the host via dipole-dipole interactions. As a result, analogous to the solution state, a polar host stabilizes the charge-transfer singlet excited state (1CT) more than the charge-transfer triplet state (3CT) [24] as well as local excited triplet state (3LE), and thus, the ΔE_{ST} value is also affected. However, the molecular kinetics are relatively restricted to a large extent in the solid phase compared to the liquid state which has greater entropy. In a recent article, Penfold et al. has revealed the influence of solid state solvation and its effect on TADF emitters based on simulation

studies [25]. Furthermore, the article reported by Monkman and coworkers clearly demonstrates the effect of host polarity on the RISC efficiency as well as the role of the host matrix to fine tune the ΔE_{ST} value [26]. In addition, Adachi and coworkers demonstrated that by controlling molecular orientation of the host, efficiency roll-off could be suppressed in a TADF-based OLED [27]. The simulation and photo-physical studies revealed that the efficiency roll-off was influenced by the hole mobility in the emission layer rather than by the optical characteristic of the devices or by the photo-physical characteristics of the TADF emitter. It was found that the host molecules oriented themselves randomly at elevated temperatures during device fabrication, which in turn reduced the hole mobility. Consequently, the recombination zone was shifted away from the interface of emission and electron transporting layers and thus, probably suppressed the efficiency roll-off. In addition, Adachi et al., demonstrated a green OLED using 1,2,3,5-tetrakis(carbazol-9-yl)-4,6-dicyanobenzene (4CzIPN) as the TADF emitter doped in a CBP host matrix which exhibited a maximum external quantum efficiency (EQE) of 19.3%. [2]

Earlier reports suggest that bipolar hosts can provide optimized charge balance and activate TADF emission of the emitter and result in greater than 20% quantum efficiency. For example, Lee et al., reported green TADF OLEDs with dicarbazole/dicarbonitrile hybridized bipolar host systems, DCzDCN [28] and mCzB-2CN [29] doped with 4CzIPN as emitter yielding high EQEs (> 25%). Another interesting bipolar host 3CzPFP composing of carbazole as donor and 3-(3-(carbazole-9-yl)phenyl) pyrido[3',2':4,5]furo[2,3-*b*]pyridine as acceptor was also reported by Lee group to achieve EQE over 30% with only 1% of 4CzIPN as emitter [17]. Another feasible approach to achieve balance charge transport is using physically blended mixture that can form exciplex as co-host system. For example,

Lee and co-workers developed a 4CzIPN-based OLED with a mixed host system composing of *N,N'*-dicarbazolyl-3,5-benzene (mCP) as donor and 1,3,5-tri[(3-pyridyl)phen-3-yl]benzene (BmPyPB) exhibits a maximum EQE of 28.6% [30]. Kim and co-workers also developed mCP: bis-4,6-(3,5-di-3-pyridylphenyl)-2-methylpyrimidine (B3PYMPM) as the exciplex-forming co-host system which can further improve the efficiency of 4CzIPN-based OLED to 29.6% [31]. These results clearly reveal the potential of using host materials with bipolar character for TADF-based OLEDs.

In this study, we report the design, synthesis and properties of a series of bipolar host materials (*o*-, *m*-, *p*-NPCz and *o*-, *m*-, *p*-NPDa) with different linking topologies of the electron-withdrawing naphthyridine as acceptor (A) [32] and the widely used electron-donating carbazole or diphenylamine as donor (D) via a phenylene bridge. By adjusting the electro-donating ability of two different kind of donors and the ortho-, meta-, or para-linking manner of the functional donor units, the physical parameters are subtly tuned. The transient photoluminescence (TRPL) decay and device performance of the hosts doped with green TADF emitter 4CzIPN are fully investigated. According to the literature [19], 4CzIPN emitter possesses a singlet/triplet energy of 2.45/2.40 eV and the energy levels (HOMO/LUMO) of -5.80/-3.40 eV. Interestingly, the emission of *o*-, *m*-, *p*-NPCz: 4CzIPN films exhibited similar spectral profile to that of 4CzIPN, whereas that of the *o*-, *m*-, *p*-NPDa: 4CzIPN films were broad and featureless. This phenomenon was attributed to diphenylamine-based hosts, *o*-, *m*-, *p*-NPDa, with lower triplet energy ($E_T= 2.22\sim 2.28$ eV) than 4CzIPN, which indicate inefficient host to dopant energy transfer. In addition, shallower HOMO/LUMO levels (-5.55~-5.48/-2.65~-2.62 eV) of *o*-, *m*-, *p*-NPDa than 4CzIPN, result in the formation of intermolecular charge transfer (CT) complex [33]. The photoluminescence quantum yields (PLQY) of *o*-, *m*-, *p*-NPCz co-deposited films are found to be much higher than *o*-, *m*-, *p*-NPDa co-deposited films. Subsequently,

the OLEDs using *o*-, *m*-, *p*-NPCz and *o*-, *m*-, *p*-NPDa as hosts were fabricated with the configuration: ITO/Tris-PCz:4% ReO₃ (60 nm)/Tris-PCz (15 nm)/Host:10 wt% 4CzIPN (25 nm)/3N-T2T (50 nm)/Liq/Al. Among these six host materials, the highest EQE (18.4%) with current efficiency (CE) of 60.8 cd/A and power efficiency (PE) of 53.8 lm/W was achieved by the ortho-interconnection of carbazole-naphthyridine, namely *o*-NPCz, which has sufficient E_T of 2.56 eV, appropriate HOMO/LUMO energy levels (-5.82/-2.7 eV), bipolar charge transport, and effective at reducing the non-radioactive decay of 4CzIPN co-deposited thin film.

2. Results and Discussions

2.1 Synthesis and Photo-physical Properties

Synthetic procedures and chemical structures of the host materials are presented in Scheme 1. The intermediates *o*-, *m*-, *p*-NPBr, naphthyridine with Br-substituted phenylene bridge, were synthesized by the condensation of 2-amino-3-pyridinecarboxaldehyde with appropriate bromoacetophenones. The *o*-, *m*-, *p*-NPBr were then connected to the electron-donating carbazole or diphenylamine moieties via palladium-catalyzed Buchwald-Hartwig amination. The materials were obtained in good yields (70~90%) after purification by column chromatography and subsequent recrystallization. The chemical structures of all intermediates and host materials were confirmed by mass, ¹H NMR and ¹³C NMR spectra, and elemental analysis. Detailed synthetic procedures are summarized in the Supporting information. All these compounds were further purified through vacuum sublimation and used for their analyses of physical properties and application as host materials of TADF-based OLEDs.

The room temperature UV-vis absorption and photoluminescence (PL) spectra in neat films of these materials are depicted in Figure 1 and the data are summarized in Table 1. The absorption band (λ_{abs}) of *o*-, *m*-, *p*-NPCz and *o*-, *m*-, *p*-NPDa were observed at 296, 296, 287, 304, 314, and 299 nm, respectively, which are assigned to the π - π^* absorption of the phenyl-substituted naphthyridine. The relatively weaker absorption of 300-350 nm was assigned to the carbazole to naphthyridine charge transfer (CT) absorption overlapped with n - π^* transition of carbazole in *o*-, *m*-, *p*-NPCz. Obviously, the CT absorption spectra of *o*-, *m*-, *p*-NPDa are rather red-shifted as compared to those of carbazole-substituted counterparts *o*-, *m*-, *p*-NPCz due to the stronger electron-donating character of diphenylamino group. It is worthy to note that the *p*-substituted cases, *p*-NPCz and *p*-NPDa, exhibit evident red-shifted

absorption peak centered at 355 and 398 nm, respectively, owing to stronger D-A interaction. The photoluminescence maximum (λ_{PL}) of *o*-, *m*-, *p*-NPCz in neat film is centered at 436, 456, and 464 nm, respectively, which is blue-shifted as compared to those diphenylamino-substituted counterparts due to the weaker electron-donating ability of carbazole group. The PL λ_{PL} of *o*-, *m*-, *p*-NPDA is located at 517, 508, and 514 nm, respectively. The E_T of *o*-, *m*-, *p*-NPCz and *o*-, *m*-, *p*-NPDA was obtained from the phosphorescence spectra recorded in neat films (10K). The *o*-, *m*-, *p*-NPCz exhibit higher E_T of 2.56-2.44 eV than E_T of *o*-, *m*-, *p*-NPDA (2.28-2.22 eV). The higher E_T of *o*-, *m*-, *p*-NPCz indicates their better potential for serving as effective host for the green TADF emitter 4CzIPN ($E_T=2.4$ eV).

2.2 Electrochemical and Thermal Properties

To obtain electrochemical properties, cyclic voltammetry technique was used to probe the redox behavior of *o*-, *m*-, *p*-NPCz and *o*-, *m*-, *p*-NPDA as well as their electrochemical stability in solutions. The cyclic voltammograms are presented in Figure 2 and the corresponding data are summarized in Table 1. The oxidation scans of *o*-, *m*-, *p*-NPCz and *o*-, *m*-, *p*-NPDA host materials were measured in dichloromethane solution (10^{-3} M) with 0.1 M tetrabutylammonium hexafluorophosphate (TBAPF₆) as supporting electrolyte and the reduction scans were performed in degassed *N,N*-dimethylformamide solution (10^{-3} M) with 0.1 M tetrabutylammonium perchlorate (TBAP) as supporting electrolyte. The irreversible oxidation potentials of *o*-, *m*-, *p*-NPCz are observed with the oxidation onset at 1.25, 1.27 and 1.26 V, respectively, which can be assigned to the typical oxidation of unprotected carbazole. The reversible reduction of the naphthyridine moiety in *o*-, *m*-, *p*-NPCz with half-way potential at 1.55, 1.52 and 1.58 V, respectively. Similarly to the cases of *o*-, *m*-, *p*-NPCz and *o*-, *m*-NPDA also showed irreversible oxidation

behavior with oxidation onset observed at 0.90 and 0.96 V respectively, which is significantly lower as compared to those of carbazole-substituted analogues, indicating the better electron-donating feature of diphenylamino group. Surprisingly, the oxidation of *p*-NPDa is *quasi*-reversible with peak centered at 1.04 V. The reversible reduction potential of *o*-, *m*-, *p*-NPDa is -1.61, -1.63 and -1.60 V, respectively, which is slightly lower as compared to the corresponding carbazole-substituted analogues. The results indicate that the electronic coupling between diphenylamino group and naphthyridine is stronger in the cases of *o*-, *m*-, *p*-NPDa, resulting in the reduced electron-accepting character of naphthyridine moiety, which is consistent with the stronger CT character observed in electronic absorption spectra.

For a practical application consideration, the HOMO levels of compounds *o*-, *m*-, *p*-NPCz and *o*-, *m*-, *p*-NPDa were determined by a photo-electron spectroscopy (AC-2) (Figure S1). The LUMO levels of compounds were then calculated by subtracting the HOMO level from the band gaps (ΔE_g) determined from the absorption edge. The HOMO/LUMO energy levels of *o*-, *m*-, *p*-NPCz are -5.82/-2.70, -5.75/-2.78, and -5.75/-2.75 eV, respectively, which may have better capability to confine the excitons within the 4CzIPN (-5.8/-3.4 eV) and thus suppress unwanted exciton-polaron quenching. In contrast, the HOMO energy levels (-5.55~-5.48 eV) of *o*-, *m*-, *p*-NPDa are relatively shallower than 4CzIPN, which might lead to the possibility of interfacial charge transfer between the 4CzIPN and *o*-, *m*-, *p*-NPDa host materials, leading to the low photoluminescence quantum yield which will be discussed later. This phenomena has also been reported by Lee's group [33]. In general, similar to the literature, the optical energy gap (E_g) and triplet energy (E_T) are shifted to longer wavelengths followed by the ortho-, meta-, para-interconnections [29,34].

The glass transition temperature (T_g) and thermal decomposition temperature

(T_d , corresponding to a 5% weight loss) of the compounds *o*-, *m*-, *p*-NPCz and *o*-, *m*-, *p*-NPDA were obtained from differential scanning calorimetry (DSC) and thermogravimetric analysis (TGA) measurements, respectively. As indicated in Table 1, *o*-, *m*-, *p*-NPCz exhibit higher morphological and thermal stabilities in terms of their T_g (76–81 °C) and T_d (281–338 °C) as compared to those of *o*-, *m*-, *p*-NPDA [T_g (54–60 °C) and T_d (244–302 °C)].

2.3 Charge Carrier Mobility

The charge-carrier transport properties of *o*-, *m*-, *p*-NPCz and *o*-, *m*-, *p*-NPDA were evaluated by measuring the carrier mobilities of their vacuum-deposited film using photoinduced time-of-flight (TOF) technique. The representative TOF transient photocurrent signals for holes and electrons were illustrated in Figure S2 and S3 (Supporting Information). Figure 3(a) depicts the obtained carrier mobilities for *o*-, *m*-, *p*-NPCz, shown as a function of the square root of the electric field. The hole mobilities varied within the range from 2×10^{-7} to 4×10^{-6} $\text{cm}^2 \text{V}^{-1}\text{s}^{-1}$ for fields varying from 3.3×10^5 to 8.3×10^5 V cm^{-1} and the electron mobilities fell within the range from 2×10^{-7} to 10^{-5} $\text{cm}^2 \text{V}^{-1}\text{s}^{-1}$ for fields varying from 2.9×10^5 to 8.3×10^5 V cm^{-1} . The field-dependence of the carrier mobilities followed the nearly universal Poole–Frenkel relationship $\mu \propto \exp(\beta E^{1/2})$ typically observed for disordered organic systems, where β is the Poole–Frenkel factor [35]. Apparently, the connecting topology has crucial influence on the charge transporting behavior. The observed hole mobilities have the trend of para > ortho > meta, whereas the electron mobilities have the trend of ortho > meta > para in NPCz case. Figure 3(b) shows the field dependence of the hole mobilities of *o*-, *m*-, *p*-NPDA. The observed hole mobilities in the range of 10^{-5} $\text{cm}^2 \text{V}^{-1}\text{s}^{-1}$ s order has the trend of para > meta > ortho in NPDA case. Unfortunately, the transient photocurrent profiles are too dispersive to enable the

clear determination of electron mobility.

2.4 Transient PL characteristics

In Figure 4, the photoluminescence decay transients and spectra of 10 wt% 4CzIPN: *o*-, *m*-, *p*-NPCz co-deposited films were conducted to ensure that the origin of observed delayed fluorescence of 4CzIPN is from TADF. *o*-, *m*-, *p*-NPCz due to its high triplet energy ($E_T = 2.56\text{-}2.44$ eV) and suitable HOMO/LUMO levels, allowing an efficient confinement of excitons within 4CzIPN. The transient PL decay characteristics of these co-deposited films show two-component decays, that is, a fast decay with a lifetime of 24.6-33.2 ns and a slow decay with a lifetime of 1.8-2.3 μs , which can be assigned to fluorescence and triplet exciton up-conversion via TADF, respectively. In addition, the PL spectra of 10 wt% 4CzIPN: *o*-, *m*-, *p*-NPCz co-deposited films showed a peak centered at ca. 535 nm and the photoluminescence quantum yield (PLQY) were measured to be 50-73% (Figure S4).

In contrast, the transient PL decay of 10 wt% 4CzIPN: *o*-, *m*-, *p*-NPDa co-deposited films were best fitted by three single exponential decay components as Figure 5 shown. The two slow decay components display one is TADF of 4CzIPN emitter and another is the formation of intermolecular CT complex (exciplex) between 4CzIPN and *o*-, *m*-, *p*-NPDa. The two overlapped and red-shift emission bands observed in the co-deposited films can be explained by the residual emission (4CzIPN) and exciplex formation, respectively, which show very low PLQYs (10-20%). In the case of 10 wt% 4CzIPN: *p*-NPDa co-deposited film, the exciplex emission peak (592 nm) is in good agreement with the energy difference (2.08 eV) between the HOMO of *p*-NPDa (-5.48 eV) and the LUMO of 4CzIPN (-3.4 eV). This result is consistent with our speculation that *o*-, *m*-, *p*-NPDa with lower E_T and shallower HOMO/LUMO levels than 4CzIPN, which indicate inefficient host to dopant energy

transfer and exciplex formation. In addition, the TRPL and spectra of *o*-, *m*-, *p*-NPDa:3N-T2T (by 1:1 weight ratio) films were measured in order to examine the possibility of exciplex formations between hosts (*o*-, *m*-, *p*-NPDa) and ETL (3N-T2T). As indicated in Figure S5, the spectra only showed the PL of *o*-, *m*-, *p*-NPDa and the decay lifetimes are in nano-second region. The result indicates no exciplex formed in the interface of host:ETL.

2.5 Electroluminescent properties

Using 10 wt% 4CzIPN doped in *o*-, *m*-, *p*-NPCz and *o*-, *m*-, *p*-NPDa films as the emitting layers (EML), multilayer OLEDs were fabricated with a configuration of ITO/4 wt% ReO₃:Tris-PCz (60 nm)/ Tris-PCz (15 nm)/ EML (25 nm)/ 3N-T2T (30 nm)/ Liq (1 nm)/Al, where 3N-T2T [36 , 37] and Liq represent 2,4,6-tris(3-(pyridin-3-yl)phenyl)-1,3,5-triazine and 8-hydroxyquinolinolitolithium. Scheme 2 shows the device structure and the schematic diagram of the energy levels of materials used in the device. To lower the hole injection barrier from ITO to Tris-PCz, we used rhenium oxides (ReO₃) as a dopant material in Tris-PCz to produce ohmic contact [38]. Tris-PCz with a high E_T (2.76 eV) and hole mobility can efficiently confine the triplet energy of EML, is selected as the HTL [34]. 3N-T2T (E_T: 2.82 eV; HOMO/LUMO: -6.77/-2.7 eV) is selected as the electron transport layer (ETL) to block the excitons within the EML.

Figure 6 depicts the electroluminescent (EL) characteristics of the *o*-, *m*-, *p*-NPCz and *o*-, *m*-, *p*-NPDa hosted devices, and the pertinent data are summarized in Table 2. Devices exhibited a lower turn-on voltage (V_{on}) of 2.0 V, excepting *o*-NPCz-based device (V_{on} of 2.4 V, high-energy barrier for hole injection from Tris-PCz to *o*-NPCz). The difference in the *J*-*V* performance is presumably because of the different hosts that influence the charge carrier transporting behavior of the EML. *o*-, *m*-,

p-NPCz-based devices display higher device efficiency than those of *o*-, *m*-, *p*-NPDA, which are consistent with previous discussion.

Among these six bipolar hosts, *o*-NPCz exhibits a higher E_T of 2.56 eV that can perform effective confinement of the 4CzIPN excitons. Therefore, *o*-NPCz-hosted device revealed the best device performance with a maximum luminance (L_{max}) of 53880 cd/m² at 11.0 V and the CIE coordinate of (0.36, 0.58). The maximum external quantum (EQE), current (CE), and power (PE) efficiencies were 18.4%, 60.8 cd/A, and 53.8 lm/W, respectively. The *m*-NPCz and *p*-NPCz hosted devices exhibited relatively lower EQEs (15.6% and 15.5%). The best performances of *o*-NPCz hosted device can be rationalized by the higher PLQY of 4CzIPN:*o*-NPCz film (0.73) than that of 4CzIPN:*m*-NPCz (0.56) and 4CzIPN:*p*-NPCz (0.56) films (Figure S4).

Quantum efficiency-luminance curves of *o*-, *m*-, *p*-NPDA hosted devices are shown in Figure 6(d), which were sharply dropped, and the EQEs were only 5.3-3.1% compared with those of *o*-, *m*-, *p*-NPCz -based devices. There are two possible reasons to explain such low EL performance of *o*-, *m*-, *p*-NPDA-hosted devices. One is lower E_T s of *o*-, *m*-, *p*-NPDA than 4CzIPN, which cannot undergo efficient energy transfer to 4CzIPN dopant. Another is the shallower HOMO levels of *o*-, *m*-, *p*-NPDA than 4CzIPN that leads to the exciplex formation between *o*-, *m*-, *p*-NPDA and 4CzIPN. The EL spectra of the devices were broad and showed yellow to orange emissions (Figure 6f).

3. Conclusion

In summary, a series of novel naphthyridine-based bipolar hosts, *o*-, *m*-, *p*-NPCz and *o*-, *m*-, *p*-NPDA, were designed and synthesized by incorporating naphthyridine unit and carbazole/diphenylamine via the ortho-, meta-, and para-position of

phenylene bridge. The optical, electrochemical properties, transient photoluminescence decay and device performances of the newly synthesized host materials were fully investigated. The pertinent compounds were used as host materials for the green TADF emitter, 4CzIPN. The photoluminescence quantum yields of *o*-, *m*-, *p*-NPCz co-deposited films are found to be much higher than *o*-, *m*-, *p*-NPDA co-deposited films. Subsequently, the green TADF-OLEDs using *o*-, *m*-, *p*-NPCz and *o*-, *m*-, *p*-NPDA as bipolar hosts were fabricated with the configuration: ITO/Tris-PCz:4% ReO₃ (60 nm)/ Tris- PCz (15 nm)/ Host: 10% 4CzIPN (25 nm)/ 3N-T2T (50 nm)/ Liq/ Al. Amongst these six host materials, the highest EQE (18.4%) with CE (60.8 cd/A) and PE (53.80 lm/W) is displayed by the ortho-interconnection of donor-acceptor, namely *o*-NPCz, which has sufficiently high triplet energy, appropriate HOMO/LUMO energy levels, and effectively reducing the non-radioactive decay of 4CzIPN co-deposited thin film. For the stronger electron-donating feature of diphenylamino groups, leads molecules *o*-, *m*-, *p*-NPDA to have higher HOMO energy levels as well as reduced optical energy gaps and triplet energies, giving less effective confinement of emissive excitons within 4CzIPN, which was verified by the observed lower PLQYs in doped films and lower EQEs from the exciplex in the devices.

Acknowledgements

The authors gratefully acknowledge financial supports from Universal Display Cooperation and Ministry of Science and Technology of Taiwan. (MOST 106-2112-M-019-002-MY3, 107-2113-M-002-019-MY3).

References

- [1] E. Ayataka, O. Mai, T. Atsushi, Y. Daisuke, K. Yoshimine, A. Chihaya, Thermally activated delayed fluorescence from Sn⁴⁺-porphyrin complexes and their application to organic light emitting diodes — a novel mechanism for electroluminescence, *Adv. Mater.* 21 (2009) 4802-4806.
- [2] H. Uoyama, K. Goushi, K. Shizu, H. Nomura, C. Adachi, Highly efficient organic light-emitting diodes from delayed fluorescence, *Nature* 492 (2012) 234.
- [3] K. Goushi, K. Yoshida, K. Sato, C. Adachi, Organic light-emitting diodes employing efficient reverse intersystem crossing for triplet-to-singlet state conversion, *Nat. Photon.* 6 (2012) 253.
- [4] Z. Yang, Z. Mao, Z. Xie, Y. Zhang, S. Liu, J. Zhao, J. Xu, Z. Chi, M.P. Aldred, Recent advances in organic thermally activated delayed fluorescence materials, *Chem. Soc. Rev.* 46 (2017) 915-1016.
- [5] Y. Liu, C. Li, Z. Ren, S. Yan, M.R. Bryce, All-organic thermally activated delayed fluorescence materials for organic light-emitting diodes, *Nat. Rev. Mater.* 3 (2018) 18020.
- [6] S. Reineke, K. Walzer, K. Leo, Triplet-exciton quenching in organic phosphorescent light-emitting diodes with Ir-based emitters, *Phys. Rev. B* 75 (2007) 125328.
- [7] M. A. Baldo, C. Adachi, S. R. Forrest, Transient analysis of organic electrophosphorescence. II. Transient analysis of triplet-triplet annihilation, *Phys. Rev. B* 62 (2000) 10967.
- [8] A. Chaskar, H.-F. Chen, K.-T. Wong, Bipolar host materials: A chemical approach for highly efficient electrophosphorescent devices, *Adv. Mater.* 23 (2011) 3876-3895.
- [9] T. Nishimoto, T. Yasuda, S.Y. Lee, R. Kondo, C. Adachi, A six-carbazole-decorated cyclophosphazene as a host with high triplet energy to realize efficient delayed-fluorescence OLEDs, *Mater. Horiz.* 1 (2014) 264-269.
- [10] I.S. Park, H. Seo, H. Tachibana, J.U. Kim, J. Zhang, S.M. Son, T. Yasuda, Cyclohexane-coupled bipolar host materials with high triplet energies for organic light-emitting diodes based on thermally activated delayed fluorescence, *ACS Appl. Mater. Interfaces* 9 (2017) 2693-2700.
- [11] D. Zhang, L. Duan, Y. Li, H. Li, Z. Bin, D. Zhang, J. Qiao, G. Dong, L. Wang, Y. Qiu, Towards high efficiency and low roll-off orange electrophosphorescent devices by fine tuning singlet and triplet energies of bipolar hosts based on indolocarbazole/1,3,5-triazine hybrids, *Adv. Funct. Mater.* 24 (2014) 3551-3561.
- [12] D. Zhang, X. Song, M. Cai, H. Kaji, L. Duan, Versatile indolocarbazole-isomer derivatives as highly emissive emitters and ideal hosts for thermally activated delayed fluorescent oleds with alleviated efficiency roll-off, *Adv. Mater.* 30 (2018) 1705406.
- [13] Y. Suzuki, Q. Zhang, C. Adachi, A solution-processable host material of 1,3-bis{3-[3-(9-carbazolyl)phenyl]-9-carbazolyl}benzene and its application in organic light-emitting diodes employing thermally activated delayed fluorescence, *J. Mater. Chem. C* 3 (2015) 1700-1706.
- [14] Y. Im, W. Song, J. Y. Lee, *J. Mater. Chem. C* 3 (2015) 8061-8065.
- [15] L.-S. Cui, S.-B. Ruan, F. Bencheikh, R. Nagata, L. Zhang, K. Inada, H. Nakanotani, L.-S. Liao, C. Adachi, *Nat. Comm.* 8 (2017) 2250.
- [16] T. Chatterjee, K.-T. Wong, Perspective on host materials for thermally activated

- delayed fluorescence organic light emitting diodes, *Adv. Optical Mater.* 7 (2019) 1800565.
- [17] D.R. Lee, B.S. Kim, C.W. Lee, Y. Im, K.S. Yook, S.-H. Hwang, J.Y. Lee, Above 30% external quantum efficiency in green delayed fluorescent organic light-emitting diodes, *ACS Appl. Mater. Interfaces* 7 (2015) 9625-9629.
- [18] S.-W. Li, C.-H. Yu, C.-L. Ko, T. Chatterjee, W.-Y. Hung, K.-T. Wong, Cyanopyrimidine–carbazole hybrid host materials for high-efficiency and low-efficiency roll-off TADF OLEDs, *ACS Appl. Mater. Interfaces* 10 (2018) 12930-12936.
- [19] W. Li, J. Li, D. Liu, Q. Jin, Simple-structured phosphorescent warm white organic light-emitting diodes with high power efficiency and low efficiency roll-off, *ACS Appl. Mater. Interfaces* 8 (2016) 22382-22391.
- [20] Y. Tao, C. Yang, J. Qin, Organic host materials for phosphorescent organic light-emitting diodes, *Chem. Soc. Rev.* 40 (2011) 2943-2970.
- [21] H. Nakanotani, K. Masui, J. Nishide, T. Shibata, C. Adachi, Promising operational stability of high-efficiency organic light-emitting diodes based on thermally activated delayed fluorescence, *Sci. Rep.* 3 (2013) 2127.
- [22] G. Méhes, K. Goushi, W.J. Potscavage, C. Adachi, Influence of host matrix on thermally-activated delayed fluorescence: Effects on emission lifetime, photoluminescence quantum yield, and device performance, *Org. Electron.* 15 (2014) 2027-2037
- [23] A.S.D. Sandanayaka, T. Matsushima, C. Adachi, Degradation mechanisms of organic light-emitting diodes based on thermally activated delayed fluorescence molecules, *J. Phys. Chem. C* 119 (2015) 23845-23851.
- [24] Q. Zhang, J. Li, K. Shizu, S. Huang, S. Hirata, H. Miyazaki, C. Adachi, Design of efficient thermally activated delayed fluorescence materials for pure blue organic light emitting diodes, *J. Am. Chem. Soc.* 134 (2012) 14706-14709.
- [25] T. Northey, J. Stacey, T.J. Penfold, The role of solid state solvation on the charge transfer state of a thermally activated delayed fluorescence emitter, *J. Mater. Chem. C* 5 (2017) 11001-11009.
- [26] P.L. dos Santos, J.S. Ward, M.R. Bryce, A.P. Monkman, Using guest–host interactions to optimize the efficiency of TADF OLEDs, *J. Phys. Chem. Lett.* 7 (2016) 3341-3346.
- [27] T. Komino, H. Nomura, T. Koyanagi, C. Adachi, Suppression of efficiency roll-off characteristics in thermally activated delayed fluorescence based organic light-emitting diodes using randomly oriented host molecules, *Chem. Mater.* 25 (2013) 3038-3047.
- [28] Y. J. Cho, K. S. Yook, J. Y. Lee, A universal host material for high external quantum efficiency close to 25% and long lifetime in green fluorescent and phosphorescent OLEDs, *Adv. Mater.* 26 (2014) 4050-4055.
- [29] C.W. Lee, J.Y. Lee, Systematic control of photophysical properties of host materials for high quantum efficiency above 25% in green thermally activated delayed fluorescent devices, *ACS Appl. Mater. Interfaces* 7 (2015) 2899-2904.
- [30] B. S. Kim, J. Y. Lee, Engineering of mixed host for high external quantum efficiency above 25% in green thermally activated delayed fluorescence device, *Adv. Funct. Mater.* 24 (2014) 3970-3977.

- [31] J. W. Sun, J.-H. Lee, C.-K. Moon, K.-H. Kim, H. Shin, J.-J. Kim, A fluorescent organic light-emitting diode with 30% external quantum efficiency, *Adv. Mater.* 26 (2014) 5684-5688.
- [32] L. Xiao, X. Xing, Z. Chen, B. Qu, H. Lan, Q. Gong, J. Kido, Highly efficient electron-transporting/injecting and thermally stable naphthyridines for organic electrophosphorescent devices, *Adv. Funct. Mater.* 23 (2013) 1323-1330.
- [33] Y. Im, J. Y. Lee, Above 20% external quantum efficiency in thermally activated delayed fluorescence device using furodipyridine-type host materials, *Chem. Mater.* 26 (2014) 1413-1419.
- [34] Y. Zhao, C. Wu, P. Qiu, X. Li, Q. Wang, J. Chen, D. Ma, New benzimidazole-based bipolar hosts: highly efficient phosphorescent and thermally activated delayed fluorescent organic light-emitting diodes employing the same device structure, *ACS Appl. Mater. Interfaces* 8 (2016) 2635-2643.
- [35] P. M. Borsenberger, D. S. Weiss, *Organic Photoreceptors for Imaging Systems*, Marcel Dekker, New York (1993).
- [36] H.-F. Chen, T.-C. Wang, S.-W. Lin, W.-Y. Hung, H.-C. Dai, H.-C. Chiu, K.-T. Wong, M.-H. Ho, T.-Y. Cho, C.-W. Chen, C.-C. Lee, Peripheral modification of 1,3,5-triazine based electron-transporting host materials for sky blue, green, yellow, red, and white electrophosphorescent devices, *J. Mater. Chem.* 22 (2012) 15620-15627.
- [37] W.-Y. Hung, T.-C. Wang, P.-Y. Chiang, B.-J. Peng, K.-T. Wong, Remote steric effect as a facile strategy for improving the efficiency of exciplex-based OLEDs, *ACS Appl. Mater. Interfaces* 9 (2017) 7355-7361.
- [38] S.J. Yoo, J.H. Chang, J.H. Lee, C.K. Moon, C.I. Wu, J.J. Kim, Formation of perfect ohmic contact at indium tin oxide/N,N'-di(naphthalene-1-yl)-N,N'-diphenyl-benzidine interface using ReO₃, *Sci. Rep.* 4 (2014) 3902.

List of Figures

Scheme 1. Molecular structures and synthesis of new bipolar host molecules *o*-, *m*-, *p*-NPCz and *o*-, *m*-, *p*-NPDA.

Figure 1. Room-temperature normalized UV-Visible absorption and PL emission spectra of *o*-, *m*-, *p*-NPCz (a,b,c) and *o*-, *m*-, *p*-NPDA (d,e,f) in neat films; phosphorescence spectra (red lines) in neat films at 10 K.

Figure 2. Cyclic voltammograms of (a) *o*-, *m*-, *p*-NPCz and (b) *o*-, *m*-, *p*-NPDA.

Figure 3. Hole and electron mobilities of (a) *o*-, *m*-, *p*-NPCz as well as hole mobilities of (b) *o*-, *m*-, *p*-NPDA with different linking positions.

Figure 4. Room-temperature transient PL decay as well as normalized UV-Vis absorption and PL emission for the 4CzIPN-doped film in (a)/(d) *o*-NPCz, (b)/(e) *m*-NPCz and (c)/(f) *p*-NPCz.

Figure 5. Room-temperature transient PL decay as well as normalized UV-Vis absorption and PL emission for the 4CzIPN-doped film in (a)/(d) *o*-NPDA, (b)/(e) *m*-NPDA and (c)/(f) *p*-NPDA.

Scheme 2. Molecular structures used in this study and an energy level diagram of the device.

Figure 6. (a)/(b) Current density-voltage-luminance (*J-V-L*) characteristics, (c)/(d) EQE and PE as a function of luminance, (e)/(f) EL spectra of *o*-, *m*-, *p*-NPCz and *o*-, *m*-, *p*-NPDA doped with 10 wt% 4CzIPN.

Table 1. Photophysical and Electrochemical Properties of *o*-, *m*-, *p*-NPCz, and *o*-, *m*-, *p*-NPDa.

Host	λ_{abs} (nm)	λ_{PL} (nm)	$^a E_{1/2}^{\text{OX}}$ (V)	$^a E_{1/2}^{\text{REV}}$ (V)	HOMO ^b (eV)	LUMO ^b (eV)	ΔE_g (eV)	E_T^c (eV)	T_g^d (°C)	T_d^d (°C)
<i>o</i> -NPCz	296,326	436	1.25	-1.55	-5.82	-2.70	3.12	2.56	80	281
<i>m</i> -NPCz	296,331	456	1.27	-1.52	-5.75	-2.78	2.97	2.46	76	296
<i>p</i> -NPCz	287,355	464	1.26	-1.58	-5.75	-2.75	3.0	2.44	81	338
<i>o</i> -NPDa	304,382	517	0.90	-1.61	-5.55	-2.63	2.92	2.28	56	244
<i>m</i> -NPDa	314,389	508	0.96	-1.63	-5.54	-2.62	2.92	2.24	54	296
<i>p</i> -NPDa	299,398	514	1.04	-1.60	-5.48	-2.65	2.83	2.22	60	302

^a $E_{1/2}^{\text{OX}}$ oxidation onset potential and $E_{1/2}^{\text{REV}}$ reduction half-wave potential are determined from cyclic voltammetry; The $E_{1/2}^{\text{OX}}$ of *p*-NPDa are calculated from its oxidation half-wave potential. ^b Determined through AC2 measurements; LUMO = HOMO + E_g ; the value of E_g was calculated from the absorption onset of the solid film. ^c Triplet energy E_T was calculated from the peak of phosphorescence spectra. ^d T_g was measured by DSC technique; T_d was determined by TGA analysis.

Table 2 EL performance of devices incorporating various host.

Host	V_{on} [V]	L_{max} [cd/m ²]	I_{max} [mA/cm ²]	EQE_{max} [%]	CE_{max} [cd/A]	PE_{max} [lm/W]	at 1000 nit [% , V]	CIE [x,y]
<i>o</i> -NPCz	2.4	53880 (11.0V)	2096	18.4	60.8	53.8	17.7, 4.4	0.36, 0.58
<i>m</i> -NPCz	2.0	74280 (11.4V)	2458	15.6	51.6	46.4	15.1, 4.4	0.33, 0.59
<i>p</i> -NPCz	2.0	51700 (10.4V)	1026	15.5	51.2	50.5	14.5, 4.8	0.34, 0.59
<i>o</i> -NPDa	2.0	7690 (8.6V)	1280	5.3	13.7	17.0	3.7, 3.8	0.42, 0.53
<i>m</i> -NPDa	2.0	5720 (9.6V)	2595	5.1%	12.3	14.9	1.9, 4.6	0.43, 0.52
<i>p</i> -NPDa	2.0	2670 (9.4V)	2451	3.1	5.6	7.9	0.6, 5.6	0.5, 0.47

^a Turn-on voltage at which emission became detectable. ^b The values of driving voltage and EQE of device at 1000 cd/m² are depicted in parentheses.

Figure 1

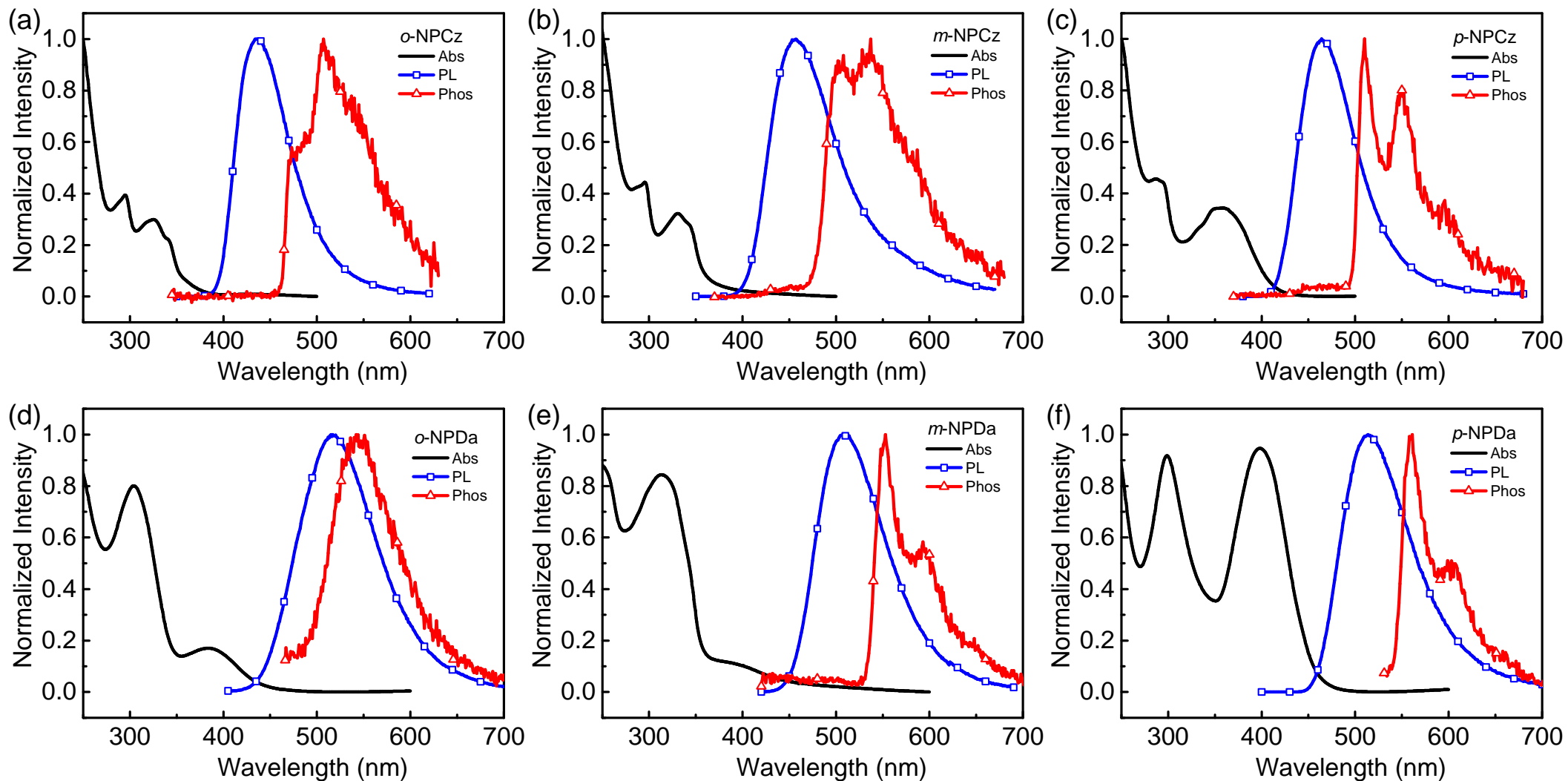


Figure 2

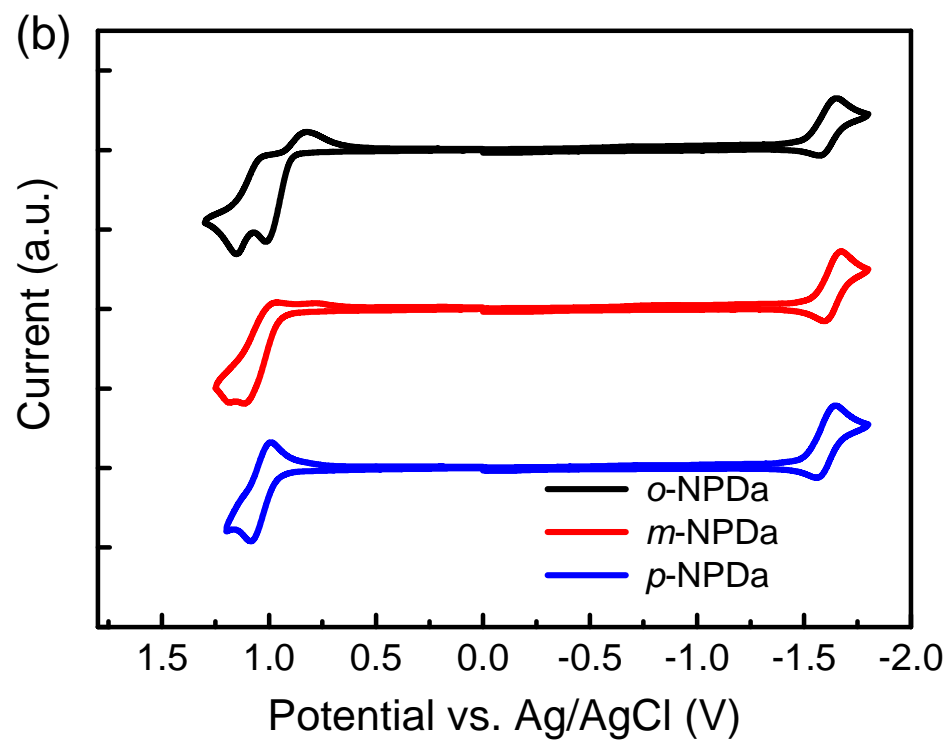
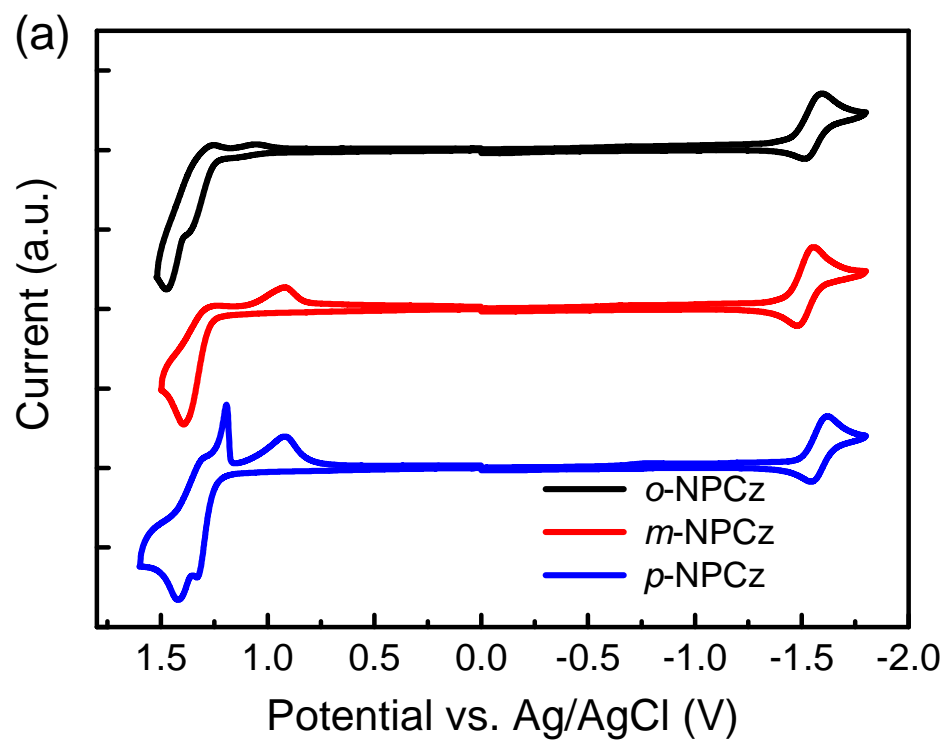


Figure 3

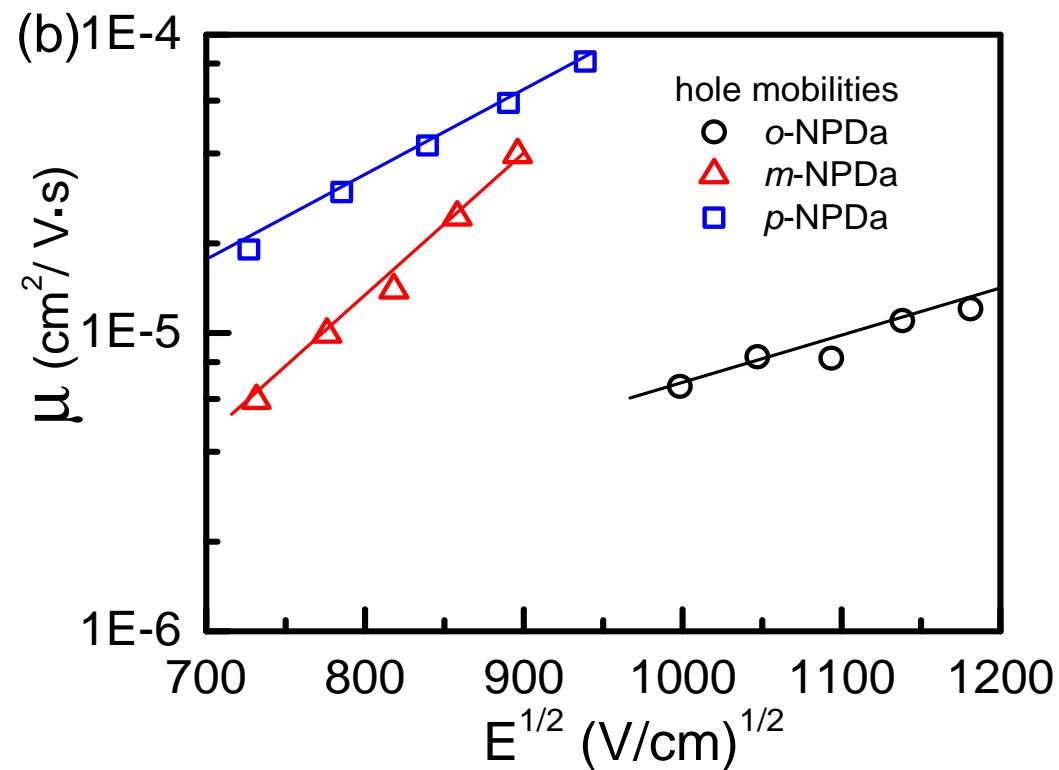
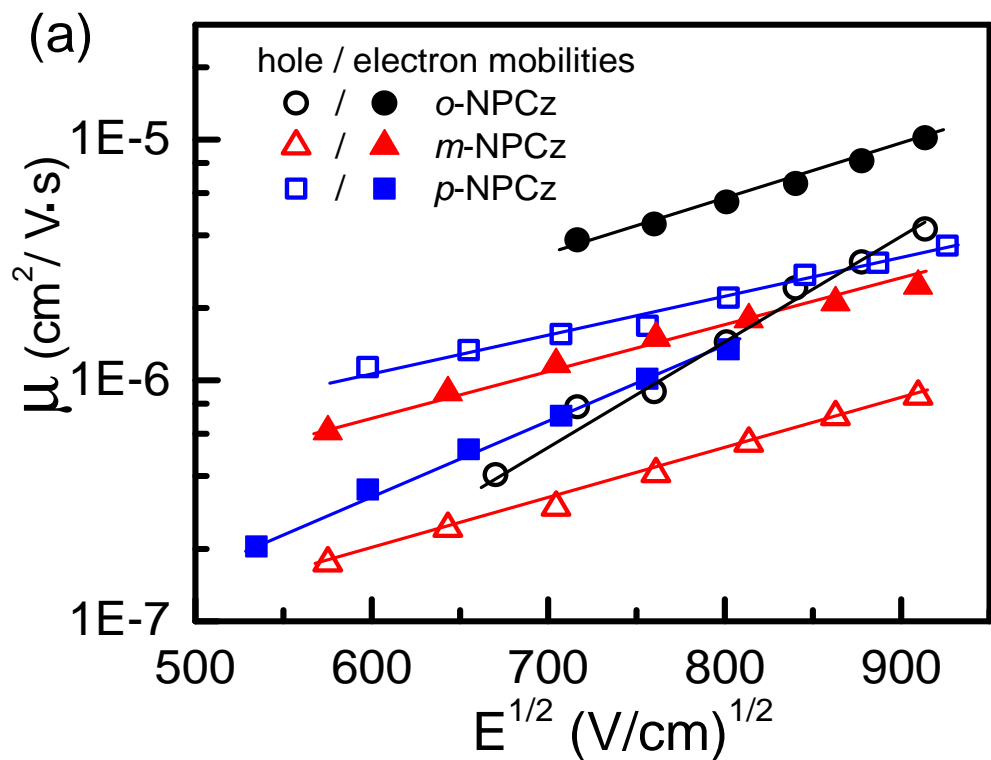


Figure 4

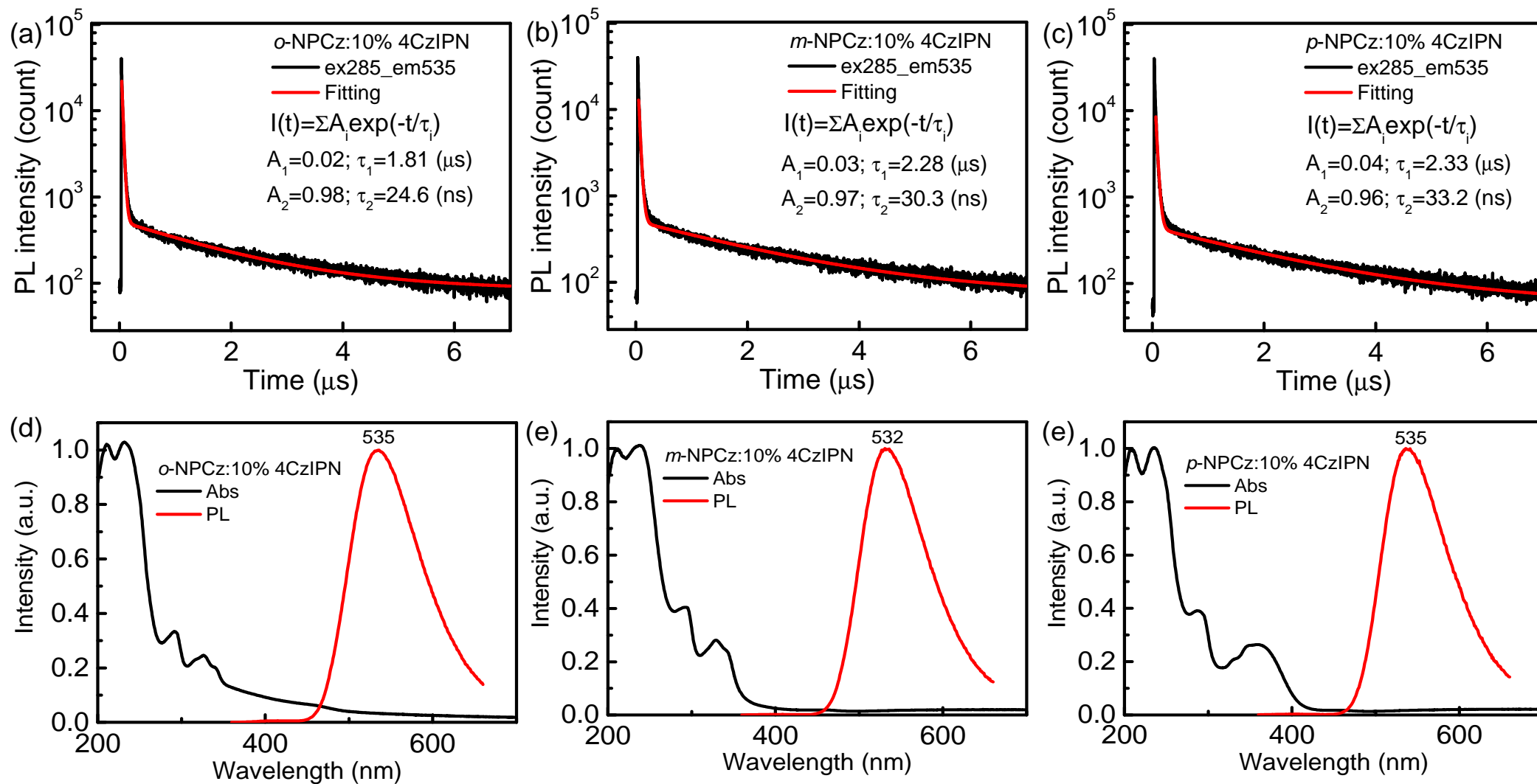


Figure 5

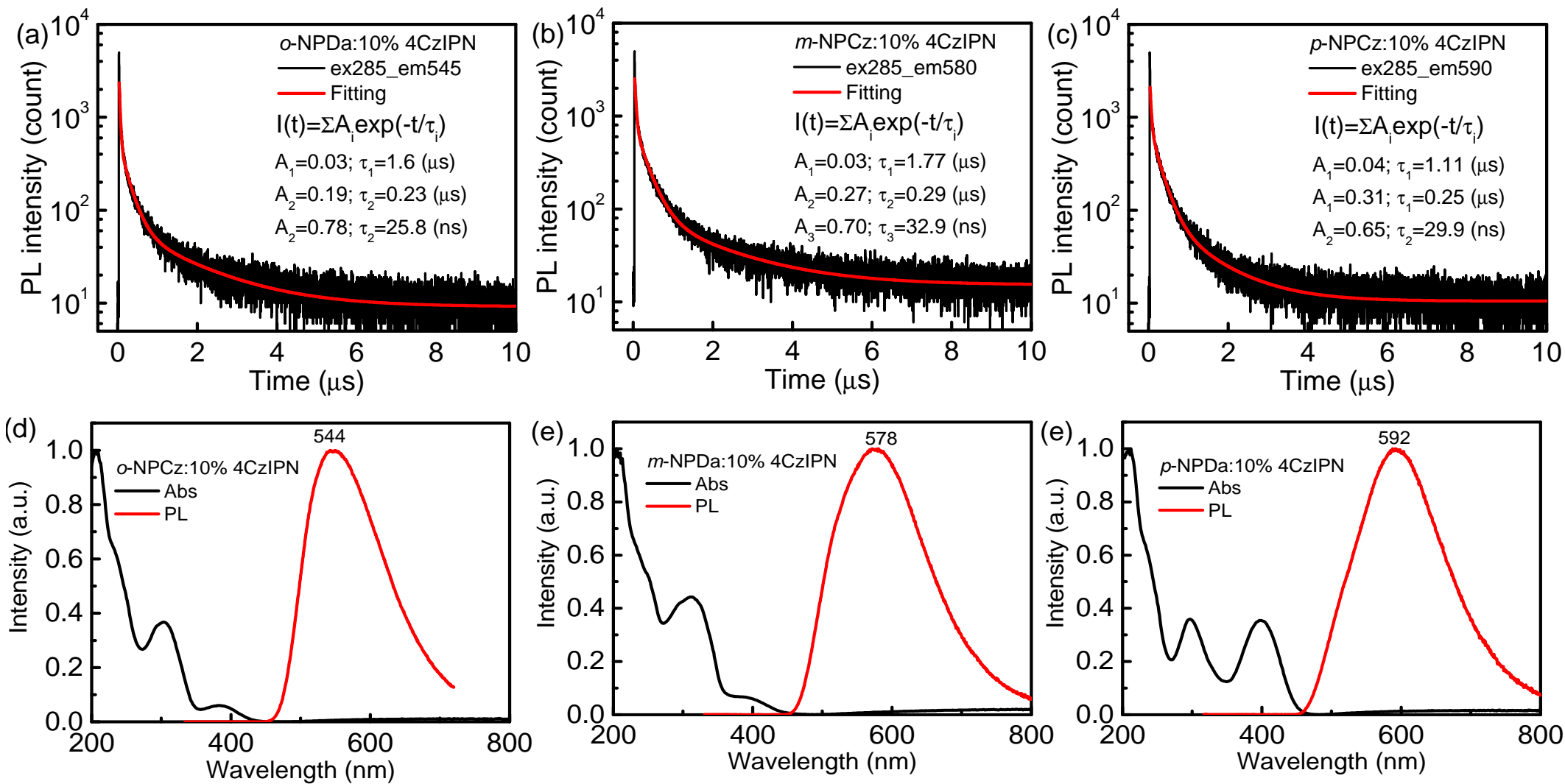
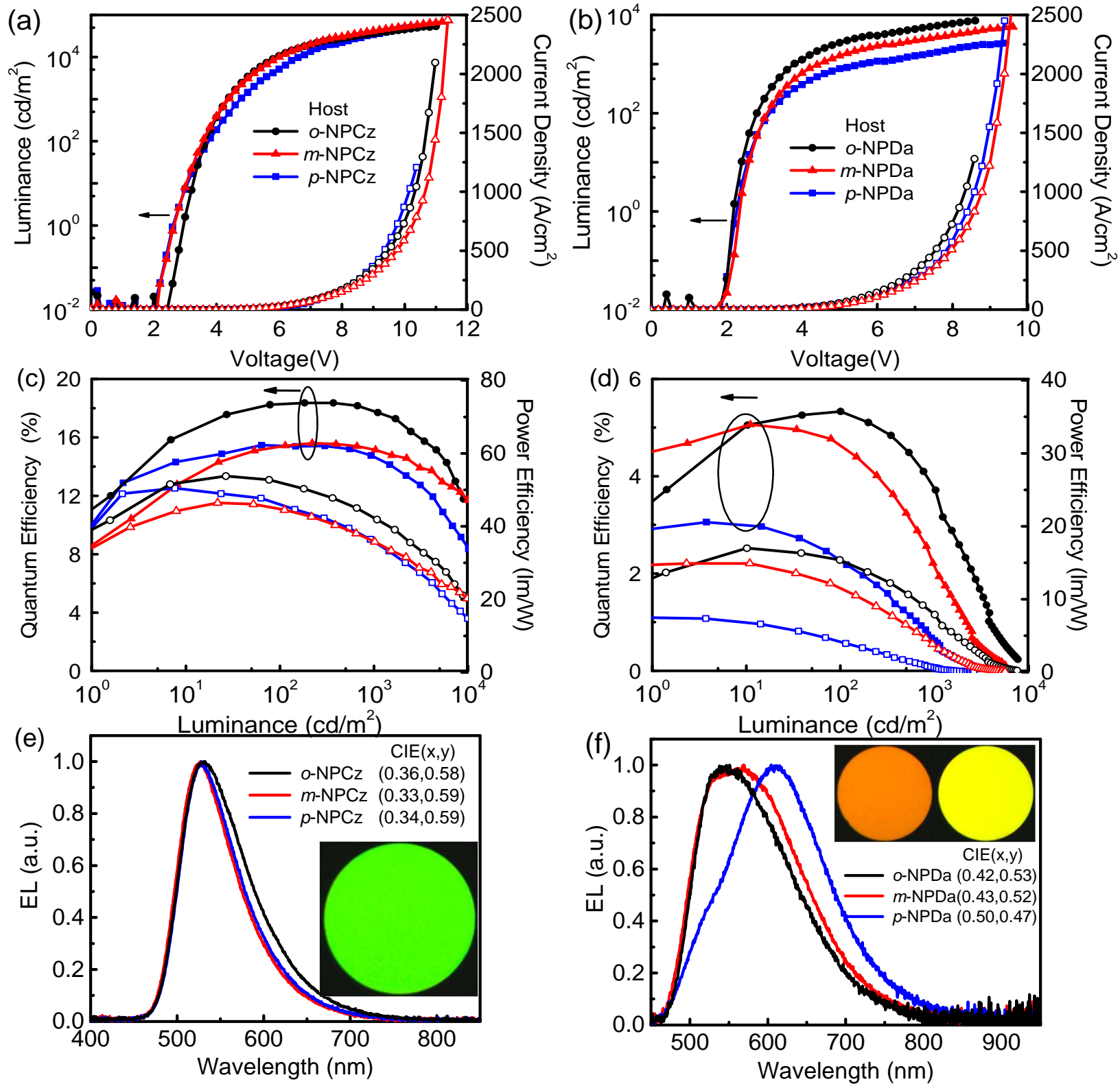
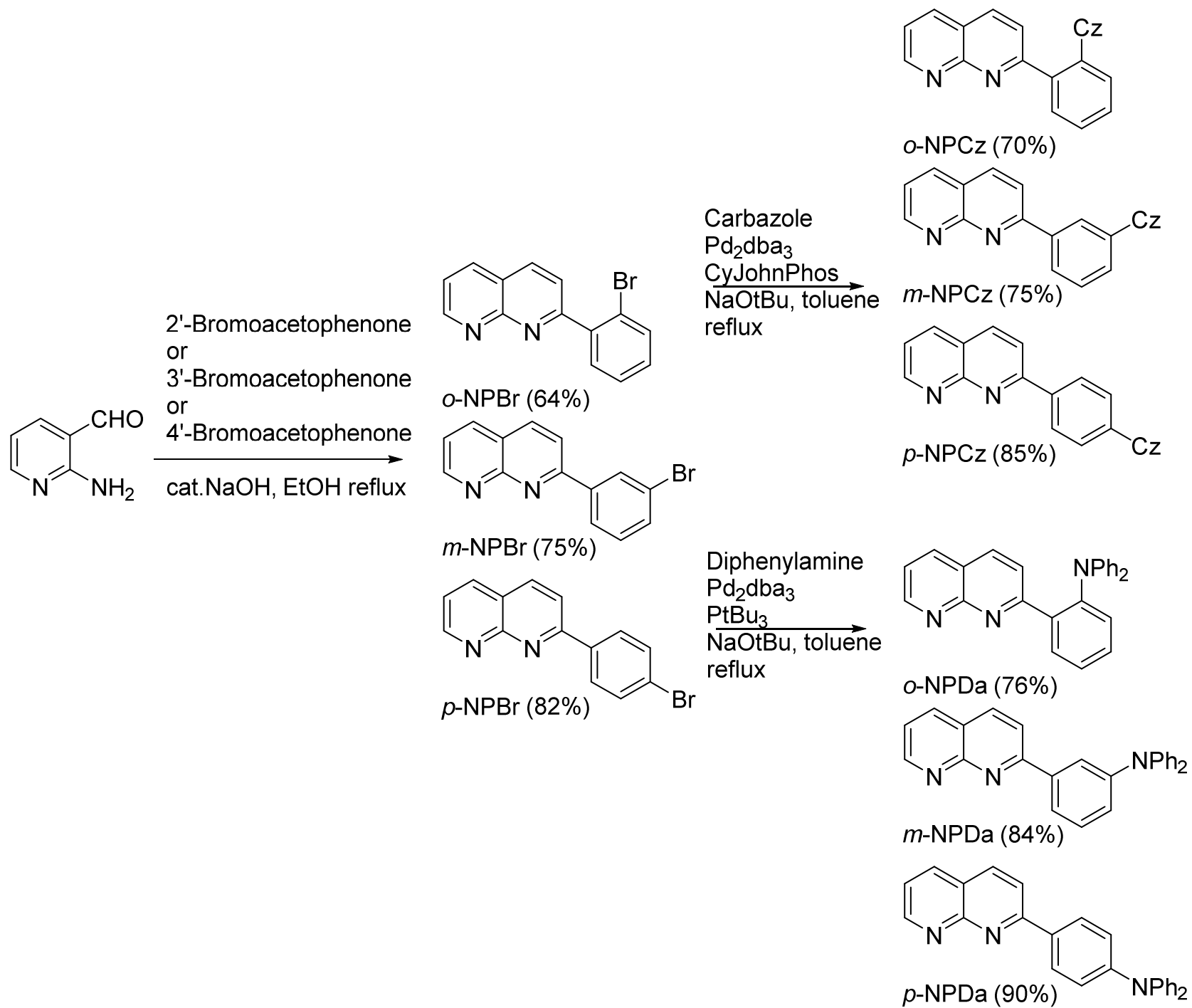


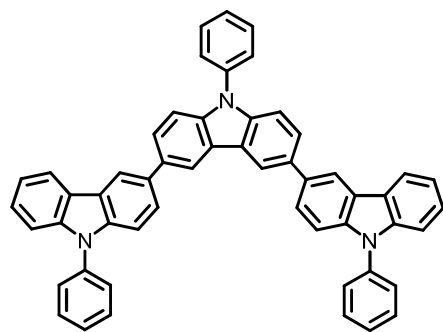
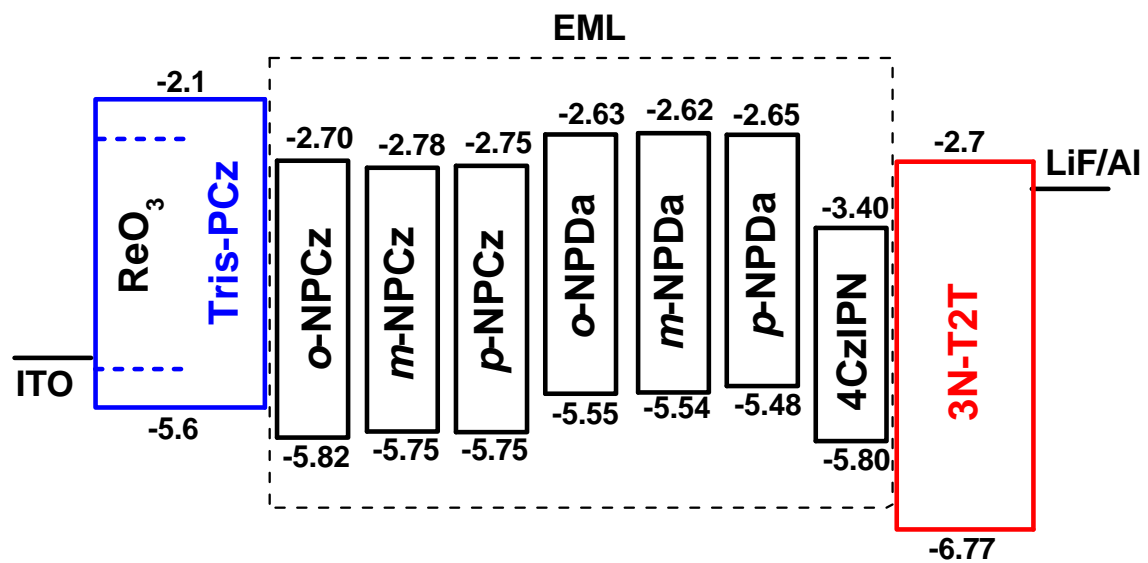
Figure 6



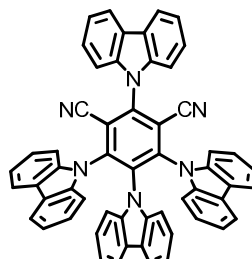
Scheme 1



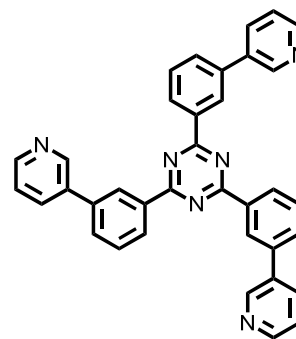
Scheme 2



Tris-PCz



4CzIPN



3N-T2T

Highlights:

- Six naphthyridine-based bipolar molecules with phenylene-bridged carbazole or diphenylamino group in different substitution way were synthesized and characterized.
- The physical properties including charge transport behavior were characterized, indicating the carbazole-based molecules are better host due to weaker charge-transfer feature.
- The application as host material of 4CzIPN in OLED was examined, in which the o-NPCz-based device exhibits the best device performance with EQE of 18.4% and low efficiency roll-off.